Microdomain Morphology of Thin ABC Triblock Copolymer Films

Hubert Elbs,[†] Kenji Fukunaga,[†] Reimund Stadler,[‡,§] Gustav Sauer,[†] Robert Magerle,[†] and Georg Krausch*[,†]

Lehrstuhl für Physikalische Chemie II, Universität Bayreuth, 95440 Bayreuth, Germany, and Lehrstuhl für Makromolekulare Chemie II, Universität Bayreuth, 95440 Bayreuth, Germany

Received August 21, 1998

ABSTRACT: We combine scanning force microscopy experiments with ex-situ swelling in different solvent vapors to investigate the microdomain structure of a thin ABC triblock copolymer film (poly(styrene-*b*-2-vinylpyridine-*b*-*tert*-butyl methacrylate)). We demonstrate that short treatment in a selective vapor and subsequent drying lead to characteristic changes in the surface morphology. The use of different solvents then allows to unambiguously identify the different phases present at the surface. This approach is established studying polymer blend and diblock copolymer thin films of known morphology. It is then applied to the a priori unknown morphology of the ABC triblock copolymer thin film. The results indicate a laterally microphase-separated polymer surface in agreement with recent theoretical considerations. The conclusions are corroborated by XPS measurements monitoring the average surface composition of the copolymer films.

1. Introduction

There has been a growing interest in the study of thin heterogeneous polymer films over the past decade, both theoretically[1] and experimentally.[2] From a fundamental viewpoint, thin films of polymer mixtures and block copolymers present advantageous model systems for the investigation of phase equilibria in reduced geometry.[3] Likewise, the influence of physical boundaries on the kinetics of phase separation and the resulting equilibrium domain morphology can be studied in quite some detail.[4] The latter is also of some importance for technological applications, as thin film multicomponent polymer systems are omnipresent in commercial products such as coatings, paints, photoresists, etc. Moreover, it has recently become clear that ultrathin films of amphiphilic block copolymers may have a large potential for lithographic purposes, as they are capable of self-organizing into highly ordered lateral structures of molecular dimensions.[5,6]

With the growing interest in such systems there has arisen the need to develop experimental tools to image heterogeneous polymer surfaces both with high spatial resolution and with chemical sensitivity. While the well-established tools of surface chemical analysis (UV and X-ray photoelectron spectroscopy, Auger electron spectroscopy, secondary ion mass spectroscopy, etc.) still lack the necessary spatial resolution,[7,8] the analytical potential of the different scanning probe microscopy techniques (scanning tunneling microscopy (STM),[9] atomic force microscopy (AFM),[10] scanning near-field optical microscopy (SNOM),[11] etc.) is still rather limited. While STM in most cases is not applicable to polymer films due to their low conductivity, the information obtained with state of the art SNOM is still unsatisfactory due to basic experimental problems.[12] Atomic force microscopy is certainly best suited to image polymer surfaces and therefore has been widely used to study polymer surfaces over the past 5 years. Novel imaging modes have been developed to adapt the technique to surfaces of organic materials and succeeded in keeping the surface damage induced by the imaging process at a minimum.[13,14] In addition, attempts have been made to combine the topographical information obtained by AFM with some sort of chemical sensitivity. This goal has been achieved via the detection of the local mechanical response of the sample[15,16] or else by use of chemically functionalized AFM tips.[17] Each of these approaches certainly has its advantages and merits; however, one has to realize that none of them provide a straightforward means of getting reliable chemical information on the surface of a heterogeneous polymer sample. This holds in particular if the chemical composition of the surface varies on molecular length scales.

In the present paper, we explore an alternative route for the identification of different polymeric phases on the surface of a heterogeneous polymer film. We use the topographic information obtained by AFM in combination with exposure of the samples to the vapor of different selective solvents. On first sight, the most straightforward way to perform such an experiment was to apply the vapor during AFM imaging and rely on the fact that the most soluble phase will take up most solvent and protrude over the remaining surface. It turns out, however, that this approach has various drawbacks. At first, the vapor treatment would have to last at least several minutes necessary to collect one or several AFM images. Depending on the nature of the solvent, this treatment could result in undesirable large-scale changes of the film morphology. In addition, practical problems may occur as parts of the AFM itself may suffer from heavy exposure to organic solvent vapors. As an alternative, one can expose the sample to the vapor of a selective solvent for a short time ex situ, dry the sample, and image the topography of the dry surface. We shall show that this procedure does reveal characteristic changes in the surface morphology useful for phase identification; however, it does *not* significantly change the overall morphology of the films. It is worth mentioning that the identification of different species at the surface of the film is based solely on well-

* Corresponding author. E-mail georg.krausch@uni-bayreuth-.de.
[†] Lehrstuhl für Physikalische Chemie II.
[‡] Lehrstuhl für Makromolekulare Chemie II.
[§] Deceased June 14, 1998.

10.1021/ma981321m CCC: $18.00
Published on Web 01/27/1999

Table 1. Molecular Parameters of the Polymers Used in the Present Study

polymer	M_w (g/mol)	M_n/M_w	φ_{PS}	φ_{P2VP}	φ_{PtBMA}
PS	371 000	1.05			
PS	803 000	1.04			
P2VP	287 000	1.06			
PtBMA	850 000	1.07			
P(S-*b*-2VP)	140 000	1.09	0.15	0.85	
P(S-*b*-2VP-*b*-tBMA)	110 000	1.08	0.17	0.24	0.59

established physicochemical properties of the polymers, i.e., their solubility in different solvents. Together with the rather artifact-free topography imaging modes in AFM, the approach suggested here allows a straightforward and model-independent analysis of thin multicomponent polymer films.

The remainder of the paper is organized as follows. After a brief description of the experimental details, we first describe experiments on thin films of different binary polymer blends of components A, B, and C. We then apply the technique to the surface of a monolayer of AB diblock copolymer micelles. In both cases, alternative experimental evidence is used to establish the (micro) domain morphology and thereby test the approach suggested here. We then apply the technique to establish the microdomain morphology of a 25 nm thick film of an incompatible ABC triblock copolymer adsorbed onto a Si wafer. The results are compared to X-ray photoelectron spectroscopy (XPS) measurements revealing the average surface composition.

2. Experimental Section

For our experiments, we used monodisperse batches of polystyrene (PS), poly(2-vinylpyridine) (P2VP), and poly(*tert*-butyl methacrylate) (PtBMA). In addition, an asymmetric P(S-*b*-2VP) diblock copolymer and a P(S-*b*-2VP-*b*-tBMA) triblock copolymer were studied. The molecular parameters of the respective polymers are summarized in Table 1. Binary mixtures of the homopolymers were dissolved in common solvents and spun-cast onto polished silicon wafers. The block copolymers were deposited onto the substrate by dip-coating from a common solvent. The Si wafers were cleaned prior to polymer deposition using standard procedures.[18] The sample surfaces were investigated by AFM using a Digital Instruments multimode AFM with a Nanoscope III controller operated in tapping mode. Film thicknesses were determined by AFM scans. To this end, the sample was scratched and the height of the remaining polymer film was determined relative to the underlying substrate. The stoichiometry of the triblock copolymer surface was investigated by XPS using a Mg Kα X-ray source ($E_{exc} = 1256.3$ eV) and a hemispherical analyzer operated at a pass energy of 202 eV.

The samples were exposed to different solvent vapors by placing them some millimeters above the liquid surface of the respective solvent kept in a beaker. All experiments were performed at room temperature. So far no attempt was undertaken to quantify the amount of solvent uptake. The exposure time was varied between 1 s and some 5 s depending on the vapor pressure of the solvent. It turned out that, for all solvents used, the exposure times were sufficient to induce the desired changes in the surface morphology of the samples without inducing detectable changes to the large-scale morphology of the films (see below). For the triblock copolymer samples, it was essential to image the same spot of the sample after treatment in different solvent vapors. To this end, the sample was scratched next to the area of interest to relocate the spot by optical microscopy during the AFM measurements.

3. Results

3.1. Polymer Blends. We start our discussion with the investigation of the surface morphology of polymer blends after spin-casting from a common solvent. This issue has been treated before in recent publications.[19,20,22] It was found that the domain morphology formed on spin-casting is accompanied by a characteristic surface structure. The domains rich in the polymer exhibiting the lower solubility in the common solvent used for spin-casting were found to protrude over the ones rich in the polymer with the higher solubility. This observation was rationalized by the fact that when the lower solubility phase solidifies, the higher solubility phase still contains some solvent. It will therefore continue to shrink on complete solvent extraction, resulting in the observed surface morphology.[20] In case of blends, an unambiguous identification of the phases can simply be achieved by selective dissolution of one of the two phases[21] or else by systematic variation of the blend composition.

In view of the task to identify the microdomain structure in the P(S-*b*-2VP-*b*-tBMA) triblock copolymer thin film, we prepared blend thin films of all binary mixtures involving two of the three homopolymers contained in the triblock copolymer. As an example, in Figure 1a is shown an AFM image of a 80/20 wt % blend thin film of PS ($M_w = 371\,000$) and P2VP ($M_w = 287\,000$) spun-cast from tetrahydrofuran (THF). The film thickness amounted to about 100 nm. The film surface is characterized by isolated protrusions of the (P2VP-rich) minority phase in a bicontinuous (PS-rich) matrix phase. The assignment of the respective polymers to the different domains is easily checked by selective dissolution of the P2VP in ethanol (not shown here). Given that THF is a better solvent for PS, the observation of protruding P2VP domains is in agreement with the notion outlined above. After imaging, the sample has been exposed for 1 s to the vapor of a better solvent for P2VP, i.e., methanol (MeOH). After this treatment, the same spot of the surface was imaged again. The surface morphology has changed markedly as can be seen in Figure 1b: The isolated domains now appear as depressions in the bicontinuous matrix phase. Other than that, no large-scale differences are observed between the two images; i.e., the overall morphology, the characteristic size, the shape, and the arrangement of the domains stay unchanged. Short treatment in THF vapor restores the original surface structure (Figure 1c).

We repeated the above experiment for PS/PtBMA and P2VP/PtBMA blends using a variety of different solvents. We consistently observe that, after vapor treatment for short times, one of two phases protrudes over the other. A qualitative summary of these results is presented schematically in Figure 2. Comparing PS and PtBMA with P2VP, we find that vapors of solvents with a rather low solubility parameter δ (cyclohexane, toluene) will lead to surface structures characterized by a P2VP-rich phase protruding over both the PS-rich and PtBMA-rich phases. After THF treatment, P2VP protrudes over PS, while PtBMA protrudes over P2VP. Solvents with a larger solubility parameter δ (dimethylformamide, methanol, chloroform), on the other hand, lead to a depression of the P2VP-rich phase with respect to both the PS-rich and PtBMA-rich phases. Comparing the latter two, vapor treatment using more polar solvents leads to PS phases protruding over PtBMA while the opposite is true for the less polar solvents.

These results indicate that short-term treatment in solvent vapor leads to surface morphologies qualitatively similar to the ones found after casting from the respective solutions.[20] It is therefore reasonable to

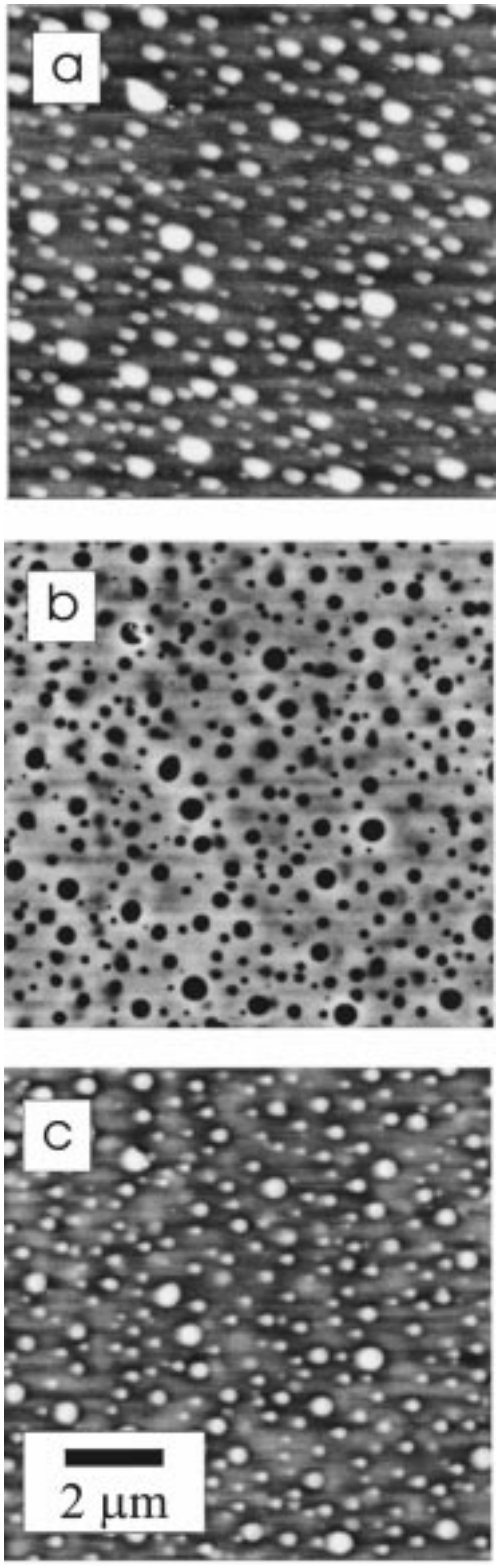

Figure 1. AFM micrographs of a 80/20 wt % blend of PS (M_w = 371 000) and P2VP (M_w = 287 000) cast from THF solution onto a polished silicon wafer (a), after subsequent treatment in MeOH vapor (b), and after subsequent treatment in THF vapor (c). The film thickness amounts to about 100 nm, and the height (depth) of the protrusions (depressions) amounts to about 10 nm.

assume that a similar mechanism is responsible for the surface structure formation. On solvent vapor exposure, both phases will take up some solvent and swell. The fact that the overall morphology of the films remains unchanged indicates that no significant miscibility is induced during this process. As the surface tension difference between the respective phases is reduced due to solvent uptake, we may assume that the surface of the swollen film will be relatively uniform and flat. Some lateral transport of chains at the phase boundaries may be necessary to achieve a flat film surface. We note that the height differences induced during this process are rather small (some tens of nanometers) compared to the lateral dimension of the domains (some microns). On drying, the lower solubility phase will solidify first while the higher solubility phase will still be able to shrink, thereby creating the observed surface morphologies.

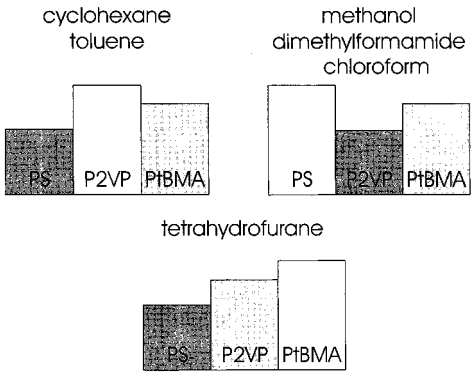

Figure 2. Schematic presentation of the relative heights observed after treatment of binary polymer blends in selective solvent vapors. The color code is the same as in the AFM images; i.e., bright areas protrude over dark areas.

3.2. Diblock Copolymer Thin Films. We now turn from polymer blend surfaces to thin films of incompatible diblock copolymers. In contrast to the micron-size domains formed in polymer blends, in the case of block copolymers the size of the domains formed on phase separation is limited to molecular length scales. As an example, we study the surface of a thin film of P(S-*b*-2VP) micelles adsorbed onto a freshly cleaved piece of mica from toluene solution. Since toluene is a poor solvent for the P2VP blocks, the polymers aggregate into spherical micelles with a P2VP core surrounded by a PS corona. As has been shown before, careful dip coating of such a solution onto a flat surface leads to the adsorption of a highly ordered monolayer of micelles.[23,24] After solvent evaporation, the micelles collapse into a 25 nm thick film consisting of flat, pancake-shaped objects. Figure 3a shows an AFM image of such a film. The surface is characterized by an ordered array of protrusions. We have recently reported AFM and transmisson electron microscopy experiments performed at the identical spot of such a sample.[25] It was demonstrated that each protrusion corresponds to a P2VP core while what appears as depression in the AFM images is due to PS. Therefore, the near surface region of the sample shown in Figure 3a exhibits a laterally inhomogeneous distribution of both PS and P2VP, resulting in a characteristic modulation of the surface topography. It is tempting to apply the vapor treatment method outlined above to test whether an inversion of protrusions and depressions can be induced in this case as well. Following this idea, we have exposed the sample shown in Figure 3a to a 1 s treatment in methanol vapor. After drying, the image shown in Figure 3b was recorded. While Figure 3a is characterized by isolated protrusions, the surface shown in Figure 3b exhibits isolated depressions in a bicontinuous, protruding matrix. Exposure to toluene vapor restores the original surface morphology (Figure 3c).

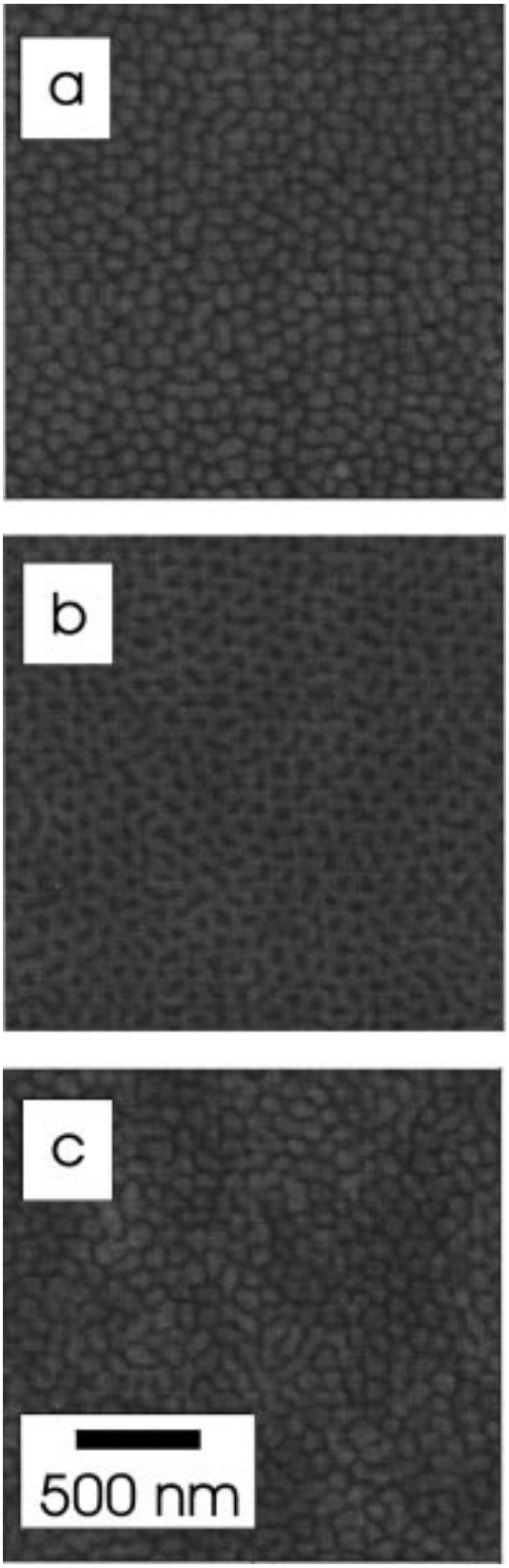

Figure 3. AFM micrograph of a 25 nm thick film of P(S-*b*-2VP) diblock copolymer adsorbed from toluene solution onto a freshly cleaved piece of mica: (a) as prepared, (b) after treatment in MeOH vapor, and (c) after treatment in toluene vapor.

While the behavior displayed in Figure 3 agrees with the results discussed above for the case of homopolymer blends on first sight, it is less obvious that the methanol treatment does not change the overall microstructure

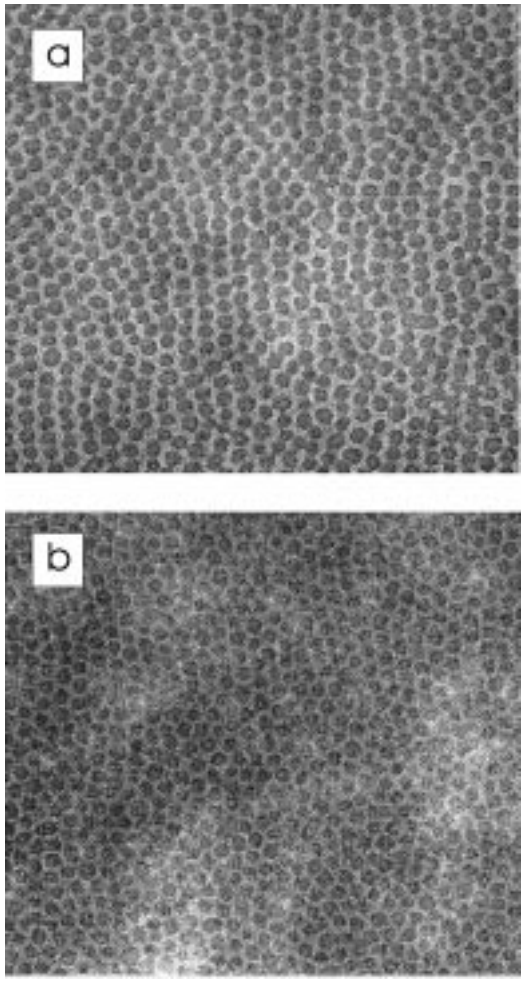

Figure 4. TEM micrographs of 25 nm thick films of P(S-*b*-2VP) diblock copolymer adsorbed from toluene solution onto carbon-coated TEM grids: (a) as prepared, (b) after treatment in MeOH vapor.

of the block copolymer film. In contrast to Figure 1, the three images displayed in Figure 3 have *not* been taken at the same spot of the sample surface. Therefore, it cannot be excluded that the micellar structure formed in toluene solution has become unstable due to MeOH vapor exposure. Since MeOH is a better solvent for the P2VP blocks, one may assume that the different surface structure shown in Figure 3b is characteristic of a different microdomain morphology in the block copolymer film. To rule out this hypothesis, we have investigated the samples before and after MeOH vapor treatment by transmission electron microscopy. To increase the contrast between the blocks, the samples were stained for 1 h in RuO_4. Figure 4a shows the TEM image taken immediately after polymer deposition from toluene solution. The image reflects the expected micellar structure of the film; i.e., it is characterized by an array of isolated (dark) P2VP microdomains embedded in a PS matrix. A second sample was produced under identical conditions and kept in MeOH vapor for some seconds and dried prior to staining. The resulting TEM image is displayed in Figure 4b. The two TEM images look nearly identical. We conclude from this experiment that the vapor treatment does *not* lead to a complex rearrangement of the copolymer chains and the formation of new aggregates. This shows that the lateral arrangement of chains is not affected by the vapor treatment,

while the surface morphology changes in a characteristic way.

The above finding suggests that treatment in selective solvent vapors for short times can also be used to determine the surface structure of block copolymer thin films. This is of particular interest as the characteristic lateral dimensions are in the 10−100 nm range, where spatially resolved chemical sensitivity is difficult to obtain with many of the conventional surface analytical techniques.

It should be noted that exposure to solvent vapor for a longer period of time indeed leads to completely different morphologies in thin diblock copolymer films. Vapor treatment in THF, for instance, eventually leads to the formation of a lamellar structure with the lamellae being oriented parallel to the substrate. It is therefore crucial to make sure that the vapor exposure times at a given vapor pressure are chosen significantly shorter than the characteristic diffusion times of polymer molecules under the respective experimental conditions. For the polymers and solvents used in the present study, we find that exposure times between 1 and 10 s at room temperature are sufficient to induce the desired changes in the surface topography without inducing any significant change in the 3D morphology of the films. A more quantitative study of these effects is presently performed and shall be presented in a forthcoming publication.

3.3. Triblock Copolymer Thin Films. We finally turn to the investigation of an a priori unknown surface structure. In an attempt to create a laterally microphase-separated polymer surface, we have investigated thin films of an incompatible ABC triblock copolymer consisting of PS, P2VP, and PtBMA.[26] As was discussed recently by Pickett and Balazs in the context of self-consistent-field calculations,[27] the thin film structure of a symmetric ABC triblock copolymer confined between two walls attracting the middle block B is expected to exhibit a lamellar microdomain structure with the lamellae being oriented perpendicular to the plane of the film. In case the attraction of the walls to the middle block is sufficiently strong, the A and C end blocks may even be expelled from the walls, resulting in homogeneous layers rich in B next to the walls and a laterally microphase-separated layer of A and C in the film center. Given that the end blocks A and C have a lower surface energy than the B middle block, one may remove one of the walls and expect that the film structure consists of a homogeneous B layer adsorbed at the substrate covered with a laterally microphase-separated surface layer of A and C.

The triblock copolymer used in our study, P(S-*b*-2VP-*b*-tBMA), fulfills most of the assumptions made by Pickett and Balazs. Indeed, the P2VP middle block is known to strongly adsorb on a polar substrate like SiO_x[28] and is expected to have a significantly higher surface energy as compared to those of PS and PtBMA.[29] Although the polymer is asymmetric ($\Phi_{PS} = 0.17$, $\Phi_{P2VP} = 0.24$, $\Phi_{PtBMA} = 0.59$), the bulk material is characterized by a distorted lamellar structure.[31] Thin films of the material were prepared by dip-coating a silicon wafer from a chloroform solution. The sample was then exposed to various solvent vapors as described above. AFM images were taken after drying. To exclude any large-scale changes in the microdomain morphology, care was taken to image the same area of the sample surface after treatment with different solvent vapors. The result of this procedure is displayed in Figure 5.

We start our discussion with the surface structure observed on a 25 nm thick film after dip-coating from $CHCl_3$ solution, followed by a 1 s treatment in THF vapor (Figure 5a). The surface is characterized by a stripelike pattern with a characteristic periodicity $d_{lat} = 60 \pm 5$ nm. The height differences are rather small and amount to about 1 nm between the center of the stripes and the areas between them. A rough inspection of the four images displayed in Figure 5 indicates that short-term exposure to different solvent vapors leads to characteristic changes in the surface morphology; however, it does not change the overall microdomain structure of the film. To explore the changes in the surface structure in more detail, it proves helpful to focus on a characteristic defect. We therefore start our discussion concentrating on the ringlike protrusion in the center of the upper right quarter of Figure 5a (arrow). What appears as protrusion after short treatment in THF vapor (Figure 5a) turns into a ringlike depression after short treatment in cyclohexane (Figure 5b). Correspondingly, the depression in the center of the ring shown in Figure 5a turns into a protrusion in Figure 5b. Comparison of parts a and b of Figure 5 shows that the vapor treatment has entirely inverted the surface topography while the characteristic features of the film remained unchanged. In addition, most of the stripelike protrusions in Figure 5b seem to be "perforated" by isolated depressions lining up along the stripe. This effect becomes even more pronounced after treatment in toluene vapor (Figure 5c). While the overall height contrast is significantly reduced, the image clearly shows an inner structure of the stripes, resulting in a characteristic length just half of the one visible in Figure 5a. Finally, treatment in MeOH vapor (Figure 5d) leads to what may be best described as an inversion of the surface structure shown in Figure 5c. In particular, what appeared as isolated depressions in Figure 5b,c now appears as isolated protrusions (see, e.g., the inner part of the ring indicated by the arrow). The structure may be characterized as a succession of continuous and broken protruding lines. The characteristic distance between them again is just half the characteristic width of the stripes displayed in Figure 5a.

We may try to summarize the results displayed in Figure 5 as follows. We observe stripelike surface corrugations after treatment in THF vapor. Treatment in cyclohexane and toluene vapors inverts the height contrast of the stripes and leads to the formation of a line of isolated depressions within each of the stripes. Finally, these structures are again inverted on treatment in MeOH vapor. We add that the observed changes in the surface morphology are reversible.

The complexity of the AFM images makes a straightforward interpretation of the results somewhat difficult. To elucidate our findings, we may assume the microdomain structure suggested by Pickett and Balazs for symmetric ABC triblock copolymer thin films as a starting point for our discussion. Given the asymmetry of the polymer and the observation of isolated microdomains, we may further assume that what should be a PS lamella may be broken up into PS microdroplets due to the short chain length of the PS block. We may then use the results obtained on the AB, BC, and CA blends discussed in section 3.1 (see Figure 2) and try to predict the surface morphology under the influence of different solvent vapors and compare it to the findings

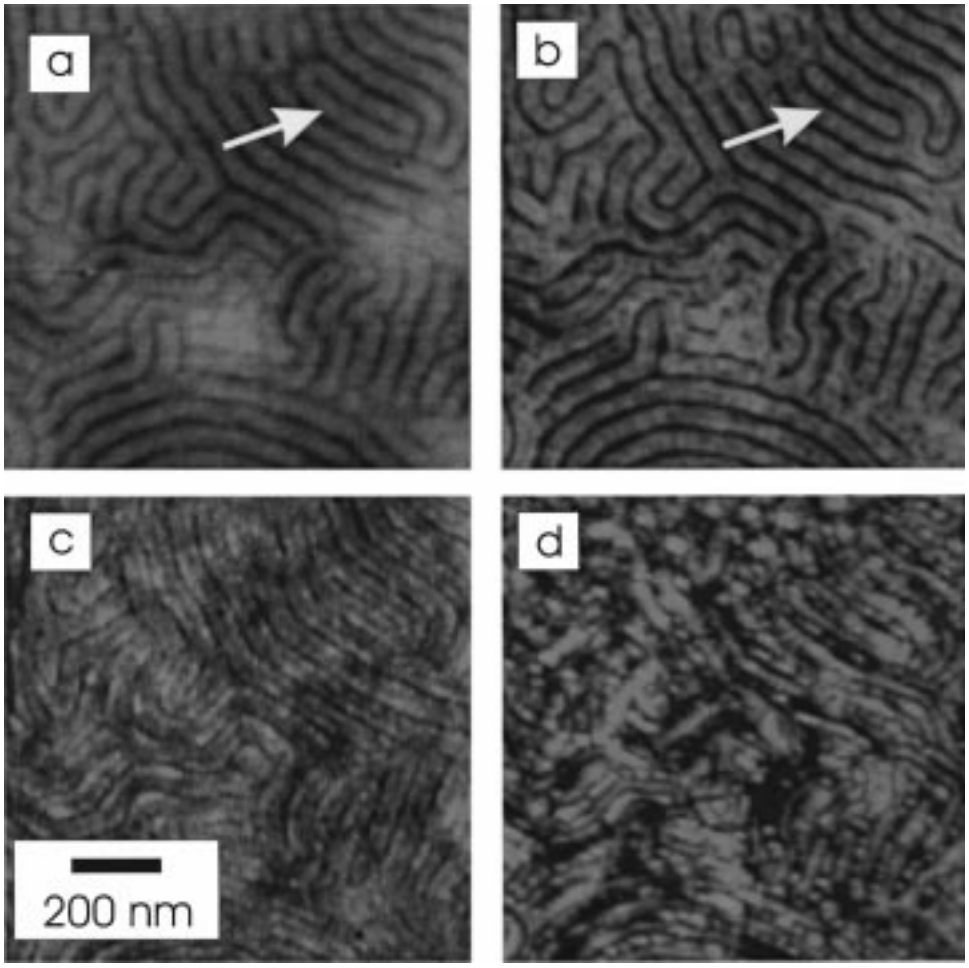

Figure 5. AFM micrographs of a 20 nm thick film of a P(S-*b*-2VP-*b*-tBMA) triblock copolymer adsorbed from solution onto a polished Si wafer: (a) after treatment in THF vapor, (b) after treatment in cyclohexane vapor, (c) after treatment in toluene vapor, and (d) after treatment in methanol vapor. The height differences amount to about 1 nm.

discussed above. We disregard for the moment a possible expulsion of the A and C blocks from the substrate and simply assume a distorted ABCBA lamellar structure with the lamellar director pointing parallel to the plane of the film. The results of this prediction are shown schematically in Figure 6 along with details of the experimental data displayed in Figure 5. Note that the gray scale of the model sketches indicate the heights resembling the color code used in the AFM images. The different blocks are identified in Figure 6a. Their lateral arrangement is believed to stay the same in all four cases. After treatment in THF vapor, the blend results (Figure 2) suggest that the PtBMA blocks protrude over the P2VP blocks, which in turn should protrude over the isolated PS microdomains. Given the large fraction of PtBMA in the block copolymer, we expect that the image is dominated by the protruding PtBMA blocks. Since PS is expected to be depressed even more than P2VP, the overall lateral periodicity is given by the distance between protruding PtBMA blocks. Experimentally, we are not able to distinguish between P2VP and PS in the grooves between neighboring PtBMA blocks. Treatment in cyclohexane vapor and toluene vapor, respectively, should change the surface morphology such that P2VP protrudes over the other two polymers (Figure 6b,c). Since PS should be depressed with respect to P2VP, we expect depressions in the P2VP protrusions for each PS microdomain. This is in agreement with the experimental observation. At the same time, the characteristic spacing of the surface topography changes to half the value characteristic of Figure 6a, since an additional line of depressions (PS) is created between neighboring (depressed) PtBMA microdomains. This is particularly obvious in the experimental data displayed in Figure 6c. Finally, the blend results displayed in Figure 2 suggest that MeOH vapor treatment (Figure 6d) leads to the formation of PtBMA protrusions (continuous) and (even higher) PS protrusions (isolated droplets) in fair agreement with the surface structure displayed in Figure 6d.

To summarize this section, we are able to interpret the data shown in Figure 5 based on the model of a distorted lamellar structure with the director being aligned parallel to the plane of the film. Consequently, we expect that all three blocks are to some extent exposed to the free surface of the polymer film. To further test this conclusion, we determined the near surface stoichiometry of the triblock copolymer film by XPS. Obviously, XPS reveals a lateral average over an area far larger than the individual microdomains. The technique should however be able to detect a possible preferential accumulation of one or two of the three blocks at the polymer surface.[30] To simplify the analysis of the triblock copolymer results, we have taken XPS spectra of the three individual homopolymers PS, P2VP, and PtBMA, respectively (Figure 7a−c). The analysis is rather straightforward, as the observed amount of nitrogen shall be characteristic for P2VP, while the intensity of the O 1s signal shall be characteristic for the amount of PtBMA in the near surface area. The

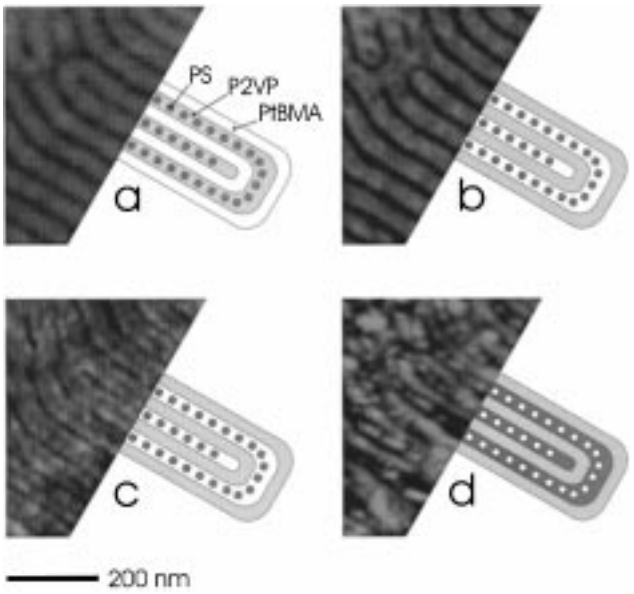

Figure 6. Schematic model of the microdomain structure in the vicinity of the ringlike defect displayed in the top right corner of Figure 5 together with experimental AFM data. The model is based on the blend results summarized in Figure 2. The color code is chosen as in the experimental images; i.e., bright areas protrude over dark areas. It *does not* identify the different blocks. The experimental data are details of the larger AFM images displayed in Figure 5. The data and the model sketches are shown for the following situations: (a) after treatment in THF vapor, (b) after treatment in cyclohexane vapor, (c) after treatment in toluene vapor, and (d) after treatment in methanol vapor. The height differences in the experimental data amount to some 1 nm.

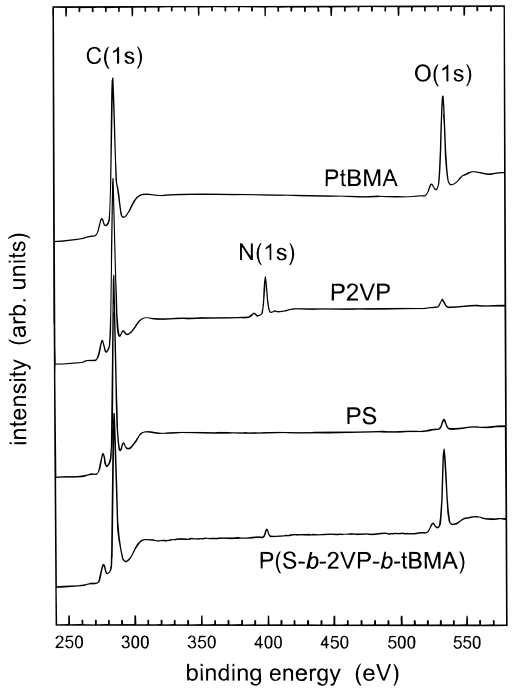

Figure 7. XPS spectra of (a) PS homopolymer, (b) P2VP homopolymer, (c) PtBMA homopolymer, and (d) a thin film of a P(S-*b*-2VP-*b*-tBMA) triblock copolymer adsorbed onto a polished silicon wafer.

situation is somewhat more complex as the polymer surfaces may be contaminated with oxygen-containing species (e.g., H_2O). This can be seen in Figure 7a,b for PS and P2VP. We have therefore determined the ratio between the integral intensities of the O 1s and the C 1s peaks observed on PS and P2VP and estimated the amount of oxygen present on the polymer surfaces. The ratios were 0.05 ± 0.01 for PS and 0.07 ± 0.01 for P2VP, respectively. Assuming a similar oxygen contamination for PtBMA and for the triblock copolymer samples, the intensities of the respective oxygen peaks were corrected accordingly. In case of PtBMA the O 1s to C 1s ratio was found to decrease strongly on X-ray exposure. This effect is known for methacrylates and is assumed to be due to degradation of the acrylic side group.[32] To correct for this effect, the O 1s to C 1s ratio was determined as a function of X-ray dose, and the zero dose value was determined by extrapolation. After these corrections, the relative amounts φ_{surf} of the three species in the near surface region of the triblock copolymer sample can be calculated from the relative peak intensities (Figure 7d). From the data shown in Figure 7d, we find $\varphi_{surf.PS} = 0.16 \pm 0.05$, $\varphi_{surf.P2VP} = 0.38 \pm 0.02$, and $\varphi_{surf.PtBMA} = 0.45 \pm 0.05$. These numbers are close to the stoichiometric values of the triblock copolymer. They indicate that all three blocks are present in the top few nanometers of the polymer sample. The XPS results therefore confirm the notion put forward on the basis of the AFM results.

4. Conclusion

In summary, we have shown that ex-situ treatment in solvent vapor and subsequent topographic imaging can be used to identify different species on a polymeric surface. We note that, in contrast to the numerous studies investigating solvent swelling of block copolymers in detail,[33] we did *not* attempt to study the equilibrium morphology characteristic of a given polymer/solvent system. On the contrary, the approach suggested here uses solvent exposure times short enough not to significantly modify a given polymeric microstructure. We have shown, however, that small changes in the surface topography of the sample can be induced by exposure to selective solvent vapors for short times. The height differences induced during this process amount to only about 5% of the characteristic size of the microdomains. We find quite generally that the phase exhibiting the lowest solubility protrudes over the higher solubility phase(s) after solvent removal. Consequently, the interpretation of the observed surface morphologies can be based on the solubility parameters of the respective polymer/solvent pairs. Since these parameters are known for many polymer/solvent pairs,[29] the suggested procedure allows a straightforward analysis of heterogeneous polymer surfaces. Moreover, as it is based on topography imaging only, it circumvents many of the problems related to the various AFM nanomechanical imaging modes.

As for the triblock copolymer studied here, we found a microdomain morphology consistent with the perpendicular ABCBA lamellar structure discussed by Pickett and Balazs[27] for the case of a selectively adsorbing middle block. The lateral periodicity ($d_{lat} = 60$ nm) observed in the thin film is in fair agreement with the small-angle X-ray scattering data obtained on bulk samples of the same polymer ($d_{bulk} = 65$ nm[31]). Despite the fact that $CHCl_3$ is a rather nonselective solvent for the particular polymer studied here, we are aware that the observed microdomain morphology may not represent the melt equilibrium of the thin film. Consequently, care has to be taken when comparing the experimental results to the theoretical calculations, which were

performed for the melt situation. For the present, we can only report qualitative agreement between the observed microstructure and the theoretical prediction for the melt. Further experiments studying the triblock copolymer thin film morphologies in more detail are under way and will be presented in a forthcoming publication.

Acknowledgment. The authors appreciate financial support through the Deutsche Forschungsgemeinschaft. The diblock copolymer used in this study was provided by E. J. Kramer. We thank E. Giebeler for synthesis and characterization of the ABC triblock copolymer. We appreciate the help of T. Goldacker and A. Göpfert during the TEM experiments. We thank V. Abetz for helpful discussions during the preparation of the manuscript.

References and Notes

(1) For a recent review, see: Binder, K. *Adv. Polym. Sci.*, in press.
(2) For a recent review, see e.g.: Krausch, G. *Mater. Sci. Eng., R* **1995**, *14*, 1.
(3) See e.g.: Kerle, T.; Klein, J.; Binder, K. *Phys. Rev. Lett.* **1996**, *77*, 1318. Lambooy, P.; Russell, T. P.; Kellog, G. J.; Mayes, A. M.; Gallagher, P. D.; Satija, S. K. *Phys. Rev. Lett.* **1994**, *72*, 2899.
(4) See, e.g.: Jones; R. A. L.; Norton, L. J.; Kramer, E. J.; Bates, F. S.; Wiltzius, P. *Phys. Rev. Lett.* **1991**, *66*, 1326. Bruder, F.; Brenn, R. *Phys. Rev. Lett.* **1992**, *69*, 624.
(5) Morkved, T. L.; Wiltzius, P.; Jaeger, H. M.; Grier, D. G.; Witten, T. A. *Appl. Phys. Lett.* **1994**, *64*, 422.
(6) Spatz, J. P.; Roescher, A.; Möller, M. *Adv. Mater.* **1996**, *8*, 337.
(7) See, e.g.: Garbassi, F.; Morra, M.; Occhiello, E. *Polymer Surfaces: From Physics to Technology*; John Wiley & Sons: Chichester, 1998.
(8) We are well aware of recent developments in photoelectron spectroscopy and X-ray microscopy, aiming to achieve chemical information with lateral resolution in the range of some 10 nm. However, while these techniques are likely to become most powerful in recent years, they require quite some machinery (synchrotron sources, expensive UHV equipment, etc.). Therefore, they are not expected to be available on an everyday basis in a typical polymer physics laboratory. (For a recent review on spectromicroscopy/microspectroscopy, see e.g.: Ade, H.; Smith, A. P.; Zhuang, G. R.; Kirz, J.; Rightor, E.; Hitchcock, A. *J. Electron Spectrosc. Relat. Phenom.* **1997**, *84*, *53*.)
(9) Binnig, G.; Rohrer, H.; Gerber, Ch.; Weibel, E. *Phys. Rev. Lett.* **1982**, *49*, 57.
(10) Binnig, G.; Quate, C. F.; Gerber, Ch. *Phys. Rev. Lett.* **1986**, *56*, 930.
(11) Pohl, D. W.; Denk, W.; Lanz, M. *Appl. Phys. Lett.* **1984**, *44*, 651.
(12) The reproducible production of suitable SNOM probes combining both high spatial resolution and high enough light transmission is still an unresolved issue. Besides this practical limitation, SNOM shall be limited to polymers containing fluorescent groups as many of the relevant polymers are transparent in the visible. For an in depth discussion of problems related to SNOM, see, e.g.: Hecht, B.; Bielefeldt, H.; Inouye, Y.; Pohl, D. W.; Novotny, L. J. *Appl. Phys.* **1997**, *81*, 2492.
(13) Zhong, Q.; et al. *Surf. Sci.* **1993**, *290*, L688.
(14) Rosa-Zeiser, A.; Weilandt, E.; Hild, S.; Marti, O. *Meas. Sci. Technol.* **1997**, *8*, 1333.
(15) Maivald, P.; Butt, H.-J.; Gould, C. B.; Prater, B.; Drake, B.; Gurley, J. A.; Ellings, J. A.; Hansma, P. K. *Nanotechnology* **1991**, *2*, 103.
(16) Krausch, G.; Hipp, M.; Böltau, M.; Marti, O.; Mlynek, J. *Macromolecules* **1995**, *28*, 260.
(17) Frisbie, C. D.; Rozsnyai, L. F.; Noy, A.; Wrighton, M.; Lieber, C. M. *Science* **1994**, *265*, 2071.
(18) The Si wafers were rinsed in organic solvents and subsequently exposed to a beam of CO_2 ice crystals ("snow jet") to remove any organic residues from the surface.
(19) Tanaka, K.; Takahara, A.; Kajiyama, T. *Macromolecules* **1996**, *29*, 3232.
(20) Walheim, S.; Böltau, M.; Mlynek, J.; Krausch, G.; Steiner, U. *Macromolecules* **1997**, *30*, 4995.
(21) Lambooy, P.; Phelan, K. C.; Haugg, O.; Krausch, G. *Phys. Rev. Lett.* **1996**, *76*, 1110.
(22) Affrosman, S.; Henn, G.; O'Neill, S. A.; Pethrick, R. A.; Stamm, M. *Macromolecules* **1996**, *29*, 5010.
(23) Li, Z.; Zhao, W.; Rafailovich, M. H.; Sokolov, J.; Khougaz, K.; Eisenberg, A.; Lennox, R. B.; Krausch, G. *J. Am. Chem. Soc.* **1996**, *118*, 10892.
(24) Meiners, J.-C.; Quintel-Ritzi, A.; Mlynek, J.; Elbs, H.; Krausch, G. *Macromolecules* **1997**, *30*, 4945.
(25) Meiners, J. C.; Elbs, H.; Ritzi, A.; Mlynek, J.; Krausch, G. *J. Appl. Phys.* **1996**, *80*, 2224.
(26) We note that first AFM experiments investigating the surface structure of a bulk ABC triblock copolymer were recently reported by Rabe and co-workers: Stocker, W.; Beckman, J.; Stadler, R.; Rabe, J. *Macromolecules* **1996**, *29*, 7502.
(27) Pickett, G. T.; Balazs, A. C. *Macromol. Theory Simul.* **1998**, *7*, 249.
(28) Tassin, J. F.; Siemens, R. L.; Tang, W. T.; Hadziioannou, G.; Swalen, J. D.; Smith, B. A. *J. Phys. Chem.* **1989**, *93*, 2106.
(29) Brandrup, J.; Immergut, E. H. *Polymer Handbook*, 3rd ed.; John Wiley and Sons: New York, 1989.
(30) We have tested the surface sensitivity of our XPS setup by investigating bilayers of P2VP and PS homopolymers with varying PS top layer thickness. We found that the escape depth of the N 1s electrons was less than 6 nm, in agreement with literature values (see, e.g.: *Handbook of X-Ray Photoelectron Spectroscopy*; Muilenberg, G. E., Ed.; Perkin-Elmer: Eden Prairie, MN, 1978).
(31) Giebeler, E. Dissertation, Universität Mainz, 1997. Giebeler, E.; Stadler, R. *Macromol. Chem. Phys.* **1997**, *198*, 3815.
(32) Briggs, D.; Hearn, S. *Spectrochim. Acta* **1985**, *40B*, 407.
(33) Albalak, R. J.; Capel, M. S.; Thomas, E. L. *Polymer* **1998**, *39*, 1647 and references therein.

MA981321M